Engineering aldo-keto reductase 1B10 to mimic the distinct 1B15 topology and specificity towards inhibitors and substrates, including retinoids and steroids

Joan Giménez-Dejoz[1], Susanne Weber[2], Álvaro Fernández-Pardo[1], Gabriele Möller[2], Jerzy Adamski[2,3,4], Sergio Porté[1], Xavier Parés[1], and Jaume Farrés[1]*

[1]Department of Biochemistry and Molecular Biology, Faculty of Biosciences, Universitat Autònoma de Barcelona, E-08193 Bellaterra (Barcelona), Spain.

[2]Research Unit Molecular Endocrinology and Metabolism, Helmholtz Zentrum München, 85764 Neuherberg, Germany.

[3]Lehrstuhl für Experimentelle Genetik, Technische Universität München, 85356 Freising-Weihenstephan, Germany.

[4]German Center for Diabetes Research, 85764 Neuherberg, Germany.

*Corresponding author: jaume.farres@uab.cat

Abstract

The aldo-keto reductase (AKR) superfamily comprises NAD(P)H-dependent enzymes that catalyze the reduction of a variety of carbonyl compounds. AKRs are classified in families and subfamilies. Humans exhibit three members of the AKR1B subfamily: AKR1B1 (aldose reductase, participates in diabetes complications), AKR1B10 (overexpressed in several cancer types), and the recently described AKR1B15. AKR1B10 and AKR1B15 share 92% sequence identity, as well as the capability of being active towards retinaldehyde. However, AKR1B10 and AKR1B15 exhibit strong differences in substrate specificity and inhibitor selectivity. Remarkably, their substrate-binding sites are the most divergent parts between them. Out of 27 residue substitutions, six are changes to Phe residues in AKR1B15. To investigate the participation of these structural changes, especially the Phe substitutions, in the functional features of each enzyme, we prepared two AKR1B10 mutants. The AKR1B10m mutant carries a segment of six AKR1B15 residues (299-304, including three Phe residues) in the respective AKR1B10 region. An additional substitution (Val48Phe) was incorporated in the second mutant, AKR1B10mF48. This resulted in structures with smaller and more hydrophobic binding pockets, more similar to that of AKR1B15. In general, the AKR1B10 mutants mirrored well the specific functional features of AKR1B15, i.e., the different preferences towards the retinaldehyde isomers, the much higher activity with steroids and ketones, and the unique behavior with inhibitors. It can be concluded that the Phe residues of loop C (299-304) contouring the substrate-binding site, in addition to Phe at position 48, strongly contribute to a narrow and more hydrophobic site in AKR1B15, which would account for its functional uniqueness. In addition, we have investigated the AKR1B10 and AKR1B15 activity toward steroids. While AKR1B10 only exhibits residual activity, AKR1B15 is an efficient 17-ketosteroid reductase. Finally, the functional role of AKR1B15 in steroid and retinaldehyde metabolism is discussed.

Highlights

- AKR1B10 and AKR1B15 widely differ in substrate specificity and inhibitor selectivity
- Substrate-binding site residues and topology are highly divergent between AKR1B enzymes
- Four Phe residues contribute to the unique kinetic properties of AKR1B15
- AKR1B15 is an efficient 9-*cis*-retinaldehyde and 17-ketosteroid reductase

Keywords

Enzyme kinetics; Inhibition; Retinaldehyde; Site-directed mutagenesis; Steroids

1. Introduction

The aldo-keto reductase (AKR) superfamily comprises NAD(P)H-dependent enzymes that catalyze the reduction of carbonyl compounds, including several physiological substrates, such as lipid peroxidation products, steroids, catecholamines, prostaglandins, and retinoids [1]. Crystallographic studies show that AKRs adopt an $(\alpha/\beta)_8$ barrel fold characterized by a deep hydrophobic substrate-binding site located near the C-terminal end. In all characterized enzymes of the superfamily, NAD(P)(H) binds first to a pocket generated by the C-terminal end of the β-sheet, at the base of a cavity forming the active-site with the conserved catalytic tetrad: Asp44, Tyr49, Lys78, and His111 (AKR1B10 residue numbering). This site interacts with the nicotinamide ring of the cofactor through a hydrogen-bonding network. The optimal substrate positioning for a specific activity is dictated by the configuration of the residues forming the substrate-binding cavity. The distinct substrate specificity and inhibitor selectivity of AKRs are given mainly by residue differences located in the external and variable loops (A, B, and C) surrounding the active-site, which have considerable plasticity [1–5].

AKRs are classified into several families (numbered 1 to 15) and subfamilies (named A to H). Humans exhibit three members of the AKR1B subfamily: AKR1B1 (the well characterized aldose reductase), AKR1B10 (aldose reductase-like) and AKR1B15. AKR1B10 reduces a wide variety of aromatic and aliphatic aldehydes, dicarbonyl compounds [6–8], and cytotoxic aldehydes (acrolein and 4-hydroxy-2-nonenal) [9], and has high catalytic efficiency with retinaldehydes [10,11]. It is up-regulated in hepatocellular carcinomas [6,12,13] and smokers' non-small cell lung carcinomas [14,15], and its elevated expression promotes proliferation of cancer cells (an alteration of its expression seems to occur even in pre-neoplastic conditions). AKR1B10 has been also reported to be overexpressed in other tumors, such as cholangiocarcinoma [13,16], pancreatic carcinoma [17], breast cancer [18–20], esophageal cancer [21], uterine carcinoma [22], nasopharyngeal carcinoma [23], as well as in skin diseases [24].

The most recently described member of the AKR1B subfamily is AKR1B15. The respective gene was predicted in a *locus* at chromosome 7 *(tcag7.1260)* within the same gene cluster as human *AKR1B1* and *AKR1B10* [25]. Recent studies have demonstrated that *AKR1B15* is an active gene, whose products are expressed *in vivo* [26]. By alternative splicing, the *AKR1B15* gene gives rise to two protein isoforms, designated as AKR1B15.1 and AKR1B15.2. The 344 amino acids comprising AKR1B15.2 has a longer N-terminus not homologous to other AKRs, does not exhibit enzymatic activity or nucleotide binding, and can be found in the cytosol. AKR1B15.1 is a 316 amino acid protein showing activity with various substrates and localizes to mitochondria [26]. The AKR1B15.1 enzyme (henceforth in this manuscript referred to as AKR1B15 for brevity) shares 92% amino acid sequence identity with AKR1B10, suggesting that both enzymes are the result of a recent gene duplication event [25]. Despite its high sequence identity with the cytosolic AKR1B10, AKR1B15 shows a distinct and broad substrate specificity [26, 27]. Particularly, ketones (including 17-ketosteroids) are good substrates for AKR1B15 while displaying low activity with AKR1B10. Importantly, AKR1B15 was also active towards retinaldehyde isomers, specially 9-*cis*-retinaldehyde, which is the best substrate for this enzyme [27], being one of the most active reductases with this retinoid isomer. The two enzymes behave also very different in terms of inhibitor selectivity [27]. An AKR1B15 structural model showed that its substrate-binding site is smaller and more hydrophobic than that of AKR1B10 [27]. Recently, a point mutation in the *AKR1B15* gene was linked to a human oxidative phosphorylation (OXPHOS) disease [28]. Another study points to *AKR1B15* as one of the new genes validated with somatic missense mutations in serous ovarian carcinoma [29]. Finally, the enzyme has been found to be up-regulated in skin diseases [24].

The sequence alignment and the structural data suggest a strong implication of residues of the loop C in the kinetic features of AKR1B15. Moreover, this loop and loop A are the sites where the majority of relevant residue changes between AKR1B10 and AKR1B15 are located.

In the present work, we designed two mutant proteins of AKR1B10. In the first mutant (AKR1B10m) we replaced six amino acid residues (299-304) within the loop C of AKR1B10, which confines the

substrate-binding site, by the respective more hydrophobic and voluminous amino acids that are present in AKR1B15. In the second mutant (AKR1B10mF48) we additionally exchanged an amino acid (Val48) located in the substrate-binding pocket of AKR1B10 by its AKR1B15 counterpart (Phe48) in order to further reduce the volume of the active site.

The purpose was to mimic in AKR1B10 the binding-site pocket of AKR1B15, with lower accessible volume as well as more rigidity, and to investigate by kinetic and structural analyses how the minimal residue changes between the two very similar proteins can provoke strong differences in their properties. Finally, the activity parameters of AKR1B15 with steroids have been determined with protein expressed and purified by a more efficient methodology [27] than the previously used [26].

2. Materials and methods

2.1. Materials

Steroids and cofactors were from Sigma-Aldrich and Serva. Radiolabeled steroids were obtained from PerkinElmer. Solvents were from Roth. Tolrestat and sorbinil were generously provided by Prof. T.G. Flynn and Pfizer, respectively. All other reagents, including substrates, were purchased from Sigma-Aldrich unless otherwise indicated.

2.2. Site-directed mutagenesis

The *AKR1B10* cDNA cloned into the bacterial expression vector pET-15b was used as the parental DNA for mutagenesis. Human *AKR1B10* was mutated using the QuickChange Lightning Site-Directed Mutagenesis Kit (Agilent Technologies). For this purpose the following primers were used: for AKR1B10m, mutation of a segment of six consecutive amino acid residues (eight nucleotide exchanges to change six amino acid residues), AKR1B10m forward primer (5'-GAAACTGGAGGGCCTTTGACTTTAAGGAATTCTCTCATTTGGAAGAC-3') and AKR1B10m reverse primer (5'-GTCTTCCAAATGAGAGAATTCCTTAAAGTCAAAGGCCCTCCAGTTTC-3'); for the additional mutation of

Val48 to Phe48 in AKR1B10mF48, AKR1B10F48 forward primer (5'-CATTGACTGTGCCTATTTCTATCAGAATGAACATG-3') and AKR1B10F48 reverse primer (5'-CATGTTCATTCTGATAGAAATAGGCACAGTCAATG-3'). The underlined regions correspond to the mutated nucleotides. The PCR steps were: *1)* DNA polymerase activation (95°C for 2 min), *2)* denaturing (95°C for 20 s), *3)* annealing (55°C for 10 s), and *4)* extension (68°C for 3 min 40 s). Steps 2-4 were repeated for 18 cycles. The PCR product was digested with *Dpn*I to eliminate the parental DNA. The resulting constructs (pET-15b-AKR1B10m and pET-AKR1B10mF48) were finally transformed into *E. coli* BL21(DE3) pLysS (Novagen) using the transformation protocol indicated by the manufacturer. Prior to expression, all mutated DNA sequences were fully sequenced to ensure that unwanted mutations were absent.

2.3. Alignment of DNA sequences, generation of the AKR1B10 mutant models, and analysis of the binding pockets

AKR1B10 and AKR1B15 sequences were gathered from the UniProt data bank and analysis was performed using the ESPript 3.0 server [30]. The crystallographic structure of AKR1B10 (PDB code: 1ZUA) [11] and the *apo*-structural model of AKR1B15 [27] were used to compare the substrate-binding site volumes of AKR1B10, AKR1B15, and the AKR1B10 mutants. The structural models of AKR1B10m and AKR1B10mF48 were generated using the Swiss-Model server [31]. The volume of the binding-site pocket was measured by using the POVME algorithm [32], whereas PyMOL was used for figure drawing.

2.4. Expression and purification of AKR1B enzymes

AKR1B10 and AKR1B15 were prepared as previously described [10,11,27]. AKR1B10m and AKR1B10mF48 were expressed as His-tagged proteins from the pET-15b vector. For mutant protein expression, transformed *E. coli* BL21(DE3) pLysS bacteria were grown in 1 L of 2xYT medium in the presence of the appropriate antibiotics at 28°C until an OD_{600} of 0.6 was reached. Protein expression was then induced by the addition of 1 mM IPTG and cells were grown for 16 h at 22°C. AKR1B10

mutant enzymes were purified as described previously for AKR1B10 [10,11] with modifications. Briefly, the purification was performed by affinity chromatography on a 5 mL nickel-charged chelating Sepharose Fast Flow column (His Trap column, GE Healthcare), using an ÄKTA FPLC (GE Healthcare) purification system. Protein was eluted by applying a stepwise concentration gradient (5, 60, 100, 250 mM) of imidazole in 50 mM Tris/HCl and 0.5 M NaCl, pH 8.0. The buffer of eluted protein fractions was exchanged by using a PD-10 column (gel filtration-desalting column, GE Healthcare). Purified His-tagged proteins were stored in 100 mM sodium phosphate, pH 7.0, at −80°C until use. Since previous work performed in our laboratory indicated that the presence of the N-terminal His-tag does not influence the kinetic constants of AKR1B enzymes (unpublished results), we used the His-tagged enzymes in our experiments.

2.5. Spectrophotometric activity assay and inhibition screening

AKR activity of wild-type and mutant enzymes was measured spectrophotometrically to follow the purification steps and to check for enzyme concentration before each kinetic experiment as previously described [10]. Briefly, standard activities were determined using D,L-glyceraldehyde as a substrate at a concentration of 6 mM for AKR1B15, 60 mM for AKR1B10 and AKR1B10mF48, and 100 mM for AKR1B10m. The activity parameters for aldehydes and ketones, with the exception of retinaldehydes and steroids, were determined following the decrease in the absorbance of the cofactor NADPH at 340 nm (ε_{340} = 6,220 $M^{-1}{\cdot}cm^{-1}$) using a Cary 400 Bio UV-Visible Spectrophotometer (Varian) [27]. Activities were analyzed in triplicates in 100 mM sodium phosphate, pH 7.0, at 25°C, using 0.2 mM NADPH in 0.2-cm path length cuvettes, with freshly prepared substrate solutions.

IC_{50} activity assays were carried out based on the quantification of the NADPH consumption that takes place when the enzyme catalyzes the conversion of glyceraldehyde into glycerol. All compounds tested for inhibition were dissolved in DMSO and assayed by the spectrophotometric activity assays in a final concentration of 0.1% (v/v) DMSO. Steady-state kinetic constant and IC_{50} (compound concentration that inhibits enzymatic activity by 50%) values were calculated by fitting the initial rates to the

appropriate equation using Grafit 5.0 (Eritacus Software) and values were given as the mean ± SEM of three experiments. When not indicated, standard error values were less than 20% of the mean values.

2.6. Enzyme activity assay with retinoids

Activity assays with retinoids were carried out using an HPLC-based methodology [33]. Briefly, retinaldehyde isomers were solubilized in glass tubes by sonication for 10 min with fatty acid-free bovine serum albumin at 1:1 molar ratio in 90 mM potassium phosphate and 40 mM potassium chloride, pH 7.4. The exact amount of solubilized retinoid was determined based on the corresponding molar absorption coefficient in aqueous solutions at the appropriate wavelength: ε_{400} = 29,500 $M^{-1}{\cdot}cm^{-1}$ for all-*trans*-retinaldehyde and ε_{367} = 26,700 $M^{-1}{\cdot}cm^{-1}$ for 9-*cis*-retinaldehyde [33]. The concentration of retinol isomers, which were used as standards of the reaction product, was determined in hexane using ε_{325} = 51,770 $M^{-1}{\cdot}cm^{-1}$ for all-*trans*-retinol [34] and ε_{325} = 43,765 $M^{-1}{\cdot}cm^{-1}$ for 9-*cis*-retinol [35]. The reactions were started by the addition of 0.2 mM cofactor and carried out for 15 min at 37°C in a final volume of 0.5 mL. With the aim to measure the steady-state enzymatic activity, the concentration of the enzymes was kept 25- to 100-fold lower than that of the substrate for all the enzymatic assays. Reactions were stopped by the addition of 1 mL of cold methanol and extracted twice with hexane.

The retinoids of the reaction mixture were dissolved in 200 µL hexane and injected onto a Nova Pak Silica column 4 µm, 3.9 x 150 mm (Waters) in hexane:methyl-*tert*-butyl ether (96:4, v/v) mobile phase at a flow rate of 2 mL/min using a Waters Alliance 2695 HPLC instrument with Waters 2996 photodiode array detector. Elution of the retinaldehyde and retinol isomers was monitored at 370 nm and 325 nm, respectively. Quantification of retinoids was performed by interpolating HPLC peak areas into a calibration curve. All retinoid manipulations were performed under dim or red light to prevent photoisomerization.

2.7. Enzyme activity assay with steroids

The conversion of steroids was analyzed by an HPLC-based method [26]. Briefly, purified enzymes were incubated with 10–20 nM ^{3}H-labeled steroid (estrone [2,4,6,7-^{3}H], androst-4-ene-3,17-dione [1,2,6,7-^{3}H], 17β-estradiol [6,7-^{3}H], or testosterone[1,2,6,7-^{3}H]), 0-15 µM unlabeled steroids and 0.6 mM NADPH (reductive reactions) or 0.7 mM $NADP^{+}$ (oxidative reactions) in 0.5 mL 100 mM sodium phosphate, 1 mM EDTA, pH 7.4, and 0.05% BSA at 37°C for 10–20 min. Reactions were stopped by the addition of 100 µL stop solution (310 mM ascorbic acid, 1% acetic acid in methanol) and extracted via solid phase extraction. Thereafter, the reactions were loaded onto conditioned (twice methanol, twice demineralized water) Strata C18-E 55 µm reversed phase (100 mg/mL) tubes (Phenomenex), washed with 500 µL demineralized water and finally eluted two times with 200 µL methanol. ^{3}H-labeled steroids were separated on a Luna 5 µm C18(2) 100 Å, 125 mm × 4 mm column (Phenomenex) using an isocratic acetonitrile:demineralized water (43:57 v/v) mobile phase at a flow rate of 1 mL/min and a Beckman Coulter HPLC system. After separation, the eluate was mixed with Quickszint Flow 302 (Zinsser Analytics) and analyzed with a Berthold radioactivity monitor. The conversion of steroids was calculated from the percentage area under the curves of the substrate and product peaks using the 32 Karat software (Beckman Coulter). Reactions were performed in triplicates and kinetic parameters were determined by fitting the conversion of steroids to the Michaelis-Menten equation using SigmaPlot version 12 software (Systat Software).

3. Results

3.1. Comparison between the structures and the substrate-binding pockets of AKR1B10 and AKR1B15

AKR1B15 exhibits a primary structure closely related to that of the well-known AKR1B10 by sharing 92% amino acid sequence identity. However, some of its properties are quite different from those of

AKR1B10, such as its substrate specificity, sensitivity to inhibitors, and reduced solubility in the bacterial expression system. Therefore, only a small number of amino acid substitutions are responsible for these functional differences. By looking at the primary sequence alignment of AKR1B10 and AKR1B15 (Fig. 1), we can identify some common characteristic features. The catalytic tetrad (Asp44, Tyr49, Lys78, and His111; numbering identical for the two enzymes) is strictly conserved, as well as the majority of loop B residues. The main differences regarding the substrate-binding pocket are found in the loops A and C. The loop A differs in four amino acid residues (Ser118, Leu122, Ala131, and Gly133 in AKR1B10 *versus* Thr118, Phe122, Met131, and Ser133 in AKR1B15) and the loop C in seven residues (Cys299, Asn300, Val301, Leu302, Gln303, Ser304, and Tyr310 in AKR1B10 *versus* Phe299, Asp300, Phe301, Lys302, Glu303, Phe304, and Phe310 in AKR1B15). The amino acid composition of these loops is thought to very much influence the topology and flexibility of the substrate-binding pocket. By comparing the crystallographic structure of AKR1B10 (PDB code: 1ZUA) with the computer model of AKR1B15 [27], and taking the volume analyses for the substrate binding pockets into account, we noticed that residues 299-304 at the end of the loop C, which is located in the external part of the pocket, play a major role in the volume difference between the substrate-binding pockets of the two enzymes. Due to the unique presence of three Phe residues (at positions 299, 301, and 304), it is very likely that this protein segment in AKR1B15 generates a substrate-binding site very different from that of AKR1B10 in terms of size and hydrophobicity. This would probably explain the observed differences between the enzymatic properties of the two enzymes. To prove this, we designed an AKR1B10 mutant, henceforth called AKR1B10m, by incorporating into the wild-type AKR1B10 six substitutions corresponding to the amino acid segment 299-304 of AKR1B15.

Figure 1. Alignment of the amino acid sequences of AKR1B10 and AKR1B15. Amino acids of the catalytic tetrads (Asp44, Tyr49, Lys78, and His111) are highlighted in red. The proline of AKR1B10 and the lysine of AKR1B15 at position 24, which have been shown to be responsible for their cytosolic and mitochondrial localization, respectively [26], are colored in blue. The serine residues at position 8, whose mutation in AKR1B15 was linked to a mitochondrial phenotype [28], are colored in green. The regions related to the mutation in AKR1B10 to mimic AKR1B15 are highlighted in yellow. Alignment obtained by using the ENDscript server [30]. (2-column fitting image)

We created a structure model of the newly designed AKR1B10m mutant and subsequently used the crystallographic structure of AKR1B10 [11] as well as the structural models of AKR1B15 [27] and AKR1B10m to compare their respective substrate-binding sites. The contour of the pocket of each protein was calculated and quite different volumes were observed. The determined volume of the cavity in AKR1B10m (158 Å^3) was sharply reduced in comparison to the one in AKR1B10 (279 Å^3) and resembled more the calculated volume of the AKR1B15 site (60 Å^3) (Fig. 2). Moreover, when the AKR1B15 and AKR1B10m models were superimposed (data not shown), it could be seen that an additional Phe in AKR1B15 (Phe48 instead of Val48 in AKR1B10) exists that participates in forming a lateral wall of the pocket. Phe48 clashes into the calculated volume sphere, indicating that it is occupying a space in the binding site of AKR1B15 and consequently contributes to the strong volume reduction of the pocket in AKR1B15 (Fig. 2).

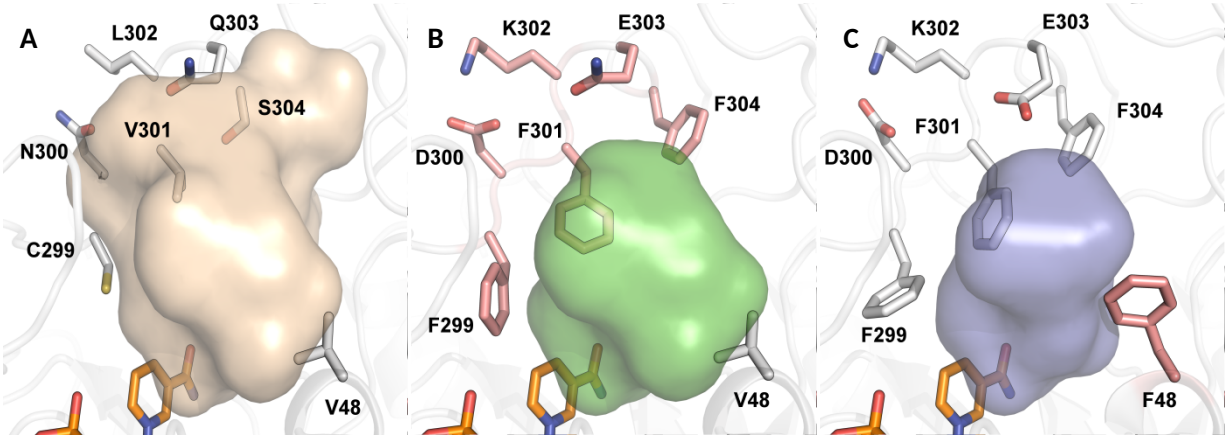

Figure 2. Comparison of the substrate-binding pockets of the (A) crystallized wild-type AKR1B10, (B) modeled AKR1B10m with the mutated residues 299 to 304, and (C) modeled AKR1B15. $NADP^+$ cofactor is displayed in orange. The surface contours of the pockets are shown in slight orange for AKR1B10, green for the AKR1B10m, and blue for AKR1B15. Mutated residues in AKR1B10m as well as the Phe48 residue in AKR1B15, implicated in further volume reduction of the pocket, are displayed in magenta. The AKR1B10m enzyme shows a reduction of the pocket volume (158 $Å^3$) when compared to AKR1B10 (279 $Å^3$) resembling more the pocket in AKR1B15 (60 $Å^3$). (2-column fitting image)

3.2. Site-directed mutagenesis

Two AKR1B10 mutants were prepared to investigate whether the residues involved in the volume restrictions would be responsible for the remarkable enzymatic differences between AKR1B10 and AKR1B15. First, we mutated six consecutive residues of loop C in AKR1B10 to their counterparts in AKR1B15: Cys299, Asn300, Val301, Leu302, Gln303, and Ser304 of AKR1B10 were substituted by Phe299, Asp300, Phe301, Lys302, Glu303, and Phe304 found in AKR1B15. This newly engineered enzyme was named AKR1B10m. With the aim of making the AKR1B10m substrate-binding site even more similar to that of AKR1B15, we substituted Val48 in AKR1B10m by a Phe48, as found in AKR1B15, and therewith generated a second mutant. This new enzyme, henceforth called AKR1B10mF48, carries the six mutations in the loop C and the additional Val48Phe substitution. The two mutant enzymes were purified to a soluble form by a procedure similar to that for the wild-type AKR1B10 and afforded 10-15 mg of purified enzyme per liter of culture. This indicates that the exchanged residues do not

cause, at least on their own, the characteristic low solubility shown by AKR1B15 during the expression and purification procedures [27].

3.3. Kinetics of AKR1B10 mutant enzymes with typical AKR substrates

The AKR1B10 mutants were designed to make the substrate-binding site of AKR1B10 more similar to that of AKR1B15. Therefore, we expected that AKR1B10m and AKR1BmF48 would show kinetic constants closer to those of AKR1B15 or at least intermediate values lying between those for the two wild-type enzymes.

The latter turned out to be the case for ketones, which are the substrate type with the most significant differences between the two wild-type AKRs. AKR1B15 efficiently uses ketones, especially long-chain compounds, such as 3-nonen-2-one. In contrast, AKR1B10 has only poor activity with these substrates (Table 1 and [27]). Interestingly, the AKR1B10 mutants were much more active with ketones, including 2,3-butanedione and 2,4-pentanedione, than the wild type AKR1B10 enzyme (Table 1). In this regard, both mutants behaved more similarly to AKR1B15 and, in consequence, it can be concluded that the substituted residues, unique for AKR1B15, are involved in the specificity of this enzyme towards ketones.

For most analyzed substrates, the two mutant enzymes showed higher k_{cat} values than the wild-type enzymes, which perhaps resulted from a change in the reaction-limiting step, which is usually the cofactor dissociation. However, the K_m values for NADPH were of the same order of magnitude for all enzymes suggesting that the mutations do not severely affect the cofactor binding.

Table 1. Kinetic parameters calculated from NADPH conversion of wild-type AKR1B10 and AKR1B15, and AKR1B10 mutants with aldehyde and ketone substrates.

Substrate	AKR1B10			AKR1B10m			AKR1B10mF48			AKR1B15[a]		
	K_m (μM)	k_{cat} (min^{-1})	k_{cat}/K_m ($mM^{-1}\cdot min^{-1}$)	K_m (μM)	k_{cat} (min^{-1})	k_{cat}/K_m ($mM^{-1}\cdot min^{-1}$)	K_m (μM)	k_{cat} (min^{-1})	k_{cat}/K_m ($mM^{-1}\cdot min^{-1}$)	K_m (μM)	k_{cat} (min^{-1})	k_{cat}/K_m ($mM^{-1}\cdot min^{-1}$)
Carbohydrate aldehydes												
D,L-glyceraldehyde	6,000[b]	35[b]	6[b]	11,620	281	24	6,600	35	6	880	10.7	12.4
Alkanals												
hexanal	112[c]	142[c]	1,300[c]	25	445	17,900	20.5	320	15,500	3.1	7.3	2,300
Ketones												
2-butanone		LA		213	71	330	46,725	68	1.5	780	10.5	13.5
3-buten-2-one		LA		3,730	380	100	12,760	123	9.7	21.3	8.2	380
3-nonen-2-one		LA		100	80	800	22.2	36.5	1,650	1.7	6.76	4,000
α-Dicarbonyls												
2,3-butanedione	540[d]	260[d]	480[d]	94	732	7,800	10.5	440	41,900	<1*	10.6	>10,600
β-Dicarbonyls												
2,4-pentanedione	58,900	8.6	0.15	2,310	162	70	2,490	28.7	11.5	40	2.2	55
3,5-heptanedione	NS	–	–	NS	–	–	NS	–	–	1,300	5.3	3.9
Cofactor												
NADPH	10[a]			21.9			12.5			5.7		

Enzymatic activities were measured spectrophotometrically by monitoring the decrease in NADPH absorbance. LA, low activity (≤ 10 mU/mg, detected at substrate concentrations that saturated AKR1B15); NS, not saturated (50 mM was the highest concentration for 3,5-heptanedione). *Approximate data because of a very low K_m value. Standard error values were less than 20% of the mean values. Data were obtained in this work or taken from references [a][27], [b][11], [c][7], and [d][36].

3.4. Kinetics of AKR1B10 mutant enzymes with retinoids

AKR1B10 and AKR1B15 are unique enzymes among the mammalian AKR1B subfamily members because they exhibit significant activity towards retinaldehyde isomers [37]. AKR1B10 specifically reduces all-*trans*-retinaldehyde with a high k_{cat} value, while AKR1B15 catalyzes the reduction of both isomers, all-*trans*-retinaldehyde and 9-*cis*-retinaldehyde, albeit with low k_{cat} values (Table 2 and [27]). The two AKR1B10 mutants are also active with the two retinaldehyde isomers.

Using all-*trans*-retinaldehyde as a substrate, both mutants displayed increased K_m values in comparison with AKR1B10. The mutant AKR1B10m showed a lower k_{cat} value (15.6 min^{-1}) than the parent enzyme (27 min^{-1}), behaving therefore more like AKR1B15 (5.4 min^{-1}). In terms of catalytic efficiencies (k_{cat}/K_m), both mutants exhibited lower values than AKR1B10 and are therefore more similar to the AKR1B15 enzyme. When using 9-*cis*-retinaldehyde as a substrate, both AKR1B10 mutants had higher K_m and k_{cat} values than the wild-type enzyme. In terms of k_{cat}/K_m, the value of AKR1B10mF48 (17,100 $mM^{-1}\cdot min^{-1}$) was much closer to that of AKR1B15 (25,600 $mM^{-1}\cdot min^{-1}$) than to that of the mutant AKR1B10m (1,200 $mM^{-1}\cdot min^{-1}$) or wild-type AKR1B10 (1,300 $mM^{-1}\cdot min^{-1}$). This indicated an important role of Phe48 in the specificity of AKR1B15 towards 9-*cis*-retinaldehyde. It is worth noticing the very high k_{cat} values of AKR1B10mF48 for both, all-*trans*- and 9-*cis*-retinaldehyde isomers (75.4 min^{-1} and 43 min^{-1}, respectively), the highest turnover rates of any AKR studied for these substrates. The sharp increase results from a single amino acid exchange (Val48Phe), since AKR1B10m exhibits much lower k_{cat} values.

Table 2. Retinaldehyde reductase activity parameters of wild-type AKR1B10 and AKR1B15, and AKR1B10 mutants.

Substrate and parameter	AKR1B10[a]	AKR1B10m	AKR1B10mF48	AKR1B15[b]
all-*trans*-retinaldehyde				
K_m (μM)	0.6 ± 0.1	6.3 ± 1.2	8.2 ± 1	1.0 ± 0.3
k_{cat} (min^{-1})	27.0 ± 1.0	15.6 ± 1.5	75.4 ± 3.8	5.4 ± 0.5
k_{cat}/K_m ($mM^{-1}·min^{-1}$)	45,000 ± 7,600	2,500 ± 550	9,180 ± 1,260	5,300 ± 1,700
9-*cis*-retinaldehyde				
K_m (μM)	0.7 ± 0.1	5 ± 1	2.5 ± 0.5	0.16 ± 0.03
k_{cat} (min^{-1})	0.9 ± 0.1	6.0 ± 0.5	43.0 ± 3.4	3.8 ± 0.2
k_{cat}/K_m ($mM^{-1}·min^{-1}$)	1,300 ± 190	1,200 ± 280	17,100 ± 3,800	25,600 ± 5,300

Enzymatic activities were measured as described in the Methods section by using an HPLC-based method. Data were obtained in this work or taken from references [a][11] and [b][27].

3.5. Kinetics with steroids

AKR1B15 is active with steroids in both reductase and dehydrogenase reactions [26]. When compared with the previous results [26], the present kinetic parameters (Table 3) differ significantly in the k_{cat} values, which are about 8-fold higher (20-fold for testosterone) than those previously determined. This can be explained by the improved expression and purification procedures used here, which allowed enzymatic assays with higher concentrations of soluble and properly folded protein, without the need for activity-impairing solubilizing agents. In contrast, the K_m values were similar to those previously reported, as expected from being independent of enzyme concentration. In addition, the current results underline that AKR1B15 prefers reductive over oxidative reactions, as previously reported [26].

Here we also report, for the first time, the detailed kinetics of AKR1B10 with C_{18} and C_{19} steroids as substrates. AKR1B10, like AKR1B15, used these substrates in both oxidative and reductive reactions. However, the AKR1B10 activity was much lower than that of AKR1B15, reflected in the very poor k_{cat} values (Table 3). It could be noticed that the catalytic efficiency of AKR1B10 with steroids was higher for the dehydrogenase than for the reductase reactions and that estrogens (C_{18} steroids) were preferred over androgens (C_{19} steroids), in contrast to the opposite preferences of AKR1B15. The AKR1B10 mutants, in general, showed higher k_{cat} and thus higher k_{cat}/K_m values than AKR1B10. In contrast to the wild-type AKR1B10 but like AKR1B15, the mutants exhibited higher preference for the

reductase than the dehydrogenase reaction. Therefore, the residue changes made the mutants closer to AKR1B15 in terms of steroid activity, suggesting that the mutated residues are involved in the very different steroid specificities of these AKR1B enzymes.

Table 3. Steroid reductase and dehydrogenase activity parameters of wild-type AKR1B10 and AKR1B15, and AKR1B10 mutants.

	Substrate and parameter	AKR1B10	AKR1B10m	AKR1B10mF48	AKR1B15
reduction	**estrone**				
	K_m (μM)	2.9 ± 0.1	13 ± 1	8.2 ± 0.9	3.0 ± 0.3
	k_{cat} (min^{-1})	0.155 ± 0.002	8.1 ± 0.4	10 ± 1	7.9 ± 0.3
	k_{cat}/K_m ($mM^{-1}·min^{-1}$)	54 ± 2	633 ± 54	1,215 ± 160	2,638 ± 256
	Δ4-androstenedione				
	K_m (μM)	4.1 ± 1.6	1.1 ± 0.1	18 ± 3	2.2 ± 0.2
	k_{cat} (min^{-1})	0.011 ± 0.002	0.62 ± 0.02	9.6 ± 1.3	8.8 ± 0.3
	k_{cat}/K_m ($mM^{-1}·min^{-1}$)	2.6 ± 1.2	560 ± 53	535 ± 128	4,090 ± 347
oxidation	**17β-estradiol**				
	K_m (μM)	1.8 ± 0.1	81 ± 11	6.8 ± 0.4	10 ± 1
	k_{cat} (min^{-1})	0.36 ± 0.01	12 ± 1	1.8 ± 0.1	4.0 ± 0.2
	k_{cat}/K_m ($mM^{-1}·min^{-1}$)	195 ± 13	147 ± 26	266 ± 18	392 ± 37
	testosterone				
	K_m (μM)	6.4 ± 0.6	12 ± 1	144 ± 44	28 ± 3
	k_{cat} (min^{-1})	0.33 ± 0.01	1.7 ± 0.1	18 ± 5	14 ± 1.2
	k_{cat}/K_m ($mM^{-1}·min^{-1}$)	52 ± 5	132 ± 12	127 ± 53	493 ± 73

Steroid conversion was measured via spiked ^{3}H-labeled steroids, as described in the Methods section by using an HPLC-based method. Data are the mean values ± SD.

3.6. Analysis of the inhibition of AKR1B10 mutants

AKR1B10 and AKR1B15 exhibit profound differences in their behavior towards typical AKR1B inhibitors, being AKR1B10 much more sensitive than AKR1B15 to most inhibitors [27]. These strong differences prompted us to measure the effect of the inhibitors on the AKR1B10 mutants (Table 4). The comparison of the inhibitory potency between the enzyme forms, measured as IC_{50} values, would provide a further tool for the analysis of their binding pockets. All compounds except for sorbinil showed an inhibitory effect on AKR1B10m. Thus, the features of AKR1B10m resembled basically the parent AKR1B10 in the inhibition assays. However, the inhibitory potency was generally much lower

for the mutant enzyme. Tolrestat, a carboxylic acid type inhibitor and one of the most potent AKR1B10 inhibitors, showed indeed a 40-fold lower potency for the mutant. As an exception, JF0064 (a non-classical aldose-reductase inhibitor), a good inhibitor for AKR1B15 (IC_{50} = 0.034 μM) but not for AKR1B10, exhibited slightly more potency against the mutant AKR1B10m (IC_{50} = 0.75 μM) than the wild-type AKR1B10 (IC_{50} = 1.0 μM). Clearly, the AKR1B10m IC_{50} values were intermediate between those of AKR1B10 and AKR1B15.

AKR1B10mF48 was significantly inhibited solely by JF0064 (IC_{50} = 0.12 μM) and epalrestat (IC_{50} = 17.1 μM). Interestingly, these two compounds were the only ones capable of having an inhibitory effect on AKR1B15 [27]. All other compounds failed to decrease the activity of this mutant enzyme, while they are inhibitors of AKR1B10m and AKR1B10. Thus, the additional single residue substitution (Val48Phe) produced a strong effect on the sensitivity towards inhibitors, resulting in the AKR1B10mF48 enzyme with inhibition properties very similar to AKR1B15 and completely different from the wild type AKR1B10.

Table 4. IC_{50} values of tested inhibitors with wild-type AKR1B10 and AKR1B15, and AKR1B10 mutants.

Inhibitor	**IC_{50} (μM)**			
	AKR1B10	**AKR1B10m**	**AKR1B10mF48**	**AKR1B15**[a]
tolrestat	0.006 ± 0.001[b]	0.26 ± 0.06	NI	NI
sorbinil	9.6 ± 0.4[c]	NI	NI	NI
JF0064	1.0 ± 0.1[d]	0.75 ± 0.12	0.120 ± 0.007	0.034 ± 0.005
epalrestat	0.330 ± 0.004[c]	2.64 ± 0.70	17.1 ± 4.0	>50
oleanolic acid	0.090 ± 0.009[e]	3.9 ± 0.9	NI	NI
sulindac	2.69 ± 0.51[f]	5.40 ± 0.76	NI	NI

The inhibitor testing was performed by using the spectrophotometric activity assay using D,L-glyceraldehyde as a substrate and NADPH as a cofactor. NI, no inhibition or IC_{50} value higher than 100 μM. Data were obtained in this work and taken from references [a][27], [b][38], [c][39], [d][40], [e][41], and [f][42].

4. Discussion

Human AKR1B10 and AKR1B15 are closely related structures sharing 92% residue identity in their sequence, and gather into an independent cluster in the evolutionary tree of the AKR1B enzymes in mammals [37]. Up to now, no orthologous proteins have been identified in mammalian model organisms such as rat, mouse, or rabbit. A unique property among the AKR1B members, which is shared by AKR1B10 and AKR1B15, is their high catalytic efficiency with retinaldehydes. While AKR1B10 is specific for the all-*trans* isomer, AKR1B15 shows a higher k_{cat}/K_m value towards 9-*cis*-retinaldehyde, similar to that of AKR1C3 [27,38]. However, the two AKR1B enzymes exhibit strong differences in their overall substrate specificity (including steroids and ketones) and inhibitor selectivity [26]. Remarkably, in spite of having two very similar primary structures, their substrate-binding pockets are the most divergent protein regions (Figs. 1 and 2). Interestingly, out of the 27 amino acid substitutions in AKR1B15 with regard to AKR1B10, six are changes to the bulky and hydrophobic Phe residues and four of them, namely Cys299Phe, Val301Phe, Ser304Phe, and Tyr310Phe, are located alone in the loop C. The presence of these voluminous residues results in the much smaller substrate-binding pocket of AKR1B15, contributing to differences in its shape and flexibility when compared to AKR1B10. These distinct structural features may be responsible for the significant differences in kinetic properties and inhibitor selectivity between the two enzymes [27].

To investigate the influence of these structural differences on the functional features of the enzymes, especially the absence or presence of Phe residues in regions defining the substrate-binding pockets, we prepared two AKR1B10 mutants: AKR1B10m and AKR1B10mF48. The AKR1B10m mutant included a 6-residue segment of AKR1B15 (amino acids 299 to 304, including three out of four Phe residues within the loop C in AKR1B15) in exchange for the respective amino acids of the AKR1B10 substrate-binding pocket. To generate AKR1B10mF48, a mutant even more similar to AKR1B15, an additional amino acid exchange (Val48Phe) was incorporated into the AKR1B10m mutant. Finally, we were able

to characterize four proteins with different substrate-binding pocket sizes: AKR1B10 with the largest, AKR1B10m and AKR1B10mF48 with intermediate, and AKR1B15 with the smallest pocket volume.

The specific functional features of AKR1B15, namely (i) the different specificity towards the retinaldehyde isomers, (ii) the much higher activity with steroids and ketones, and (iii) the unique behavior with inhibitors, could be, in general, well reproduced in the AKR1B10 mutants, especially in the AKR1B10mF48 mutant containing seven substituted residues. It can be concluded that the Phe residues of loop C contouring the binding site, in addition to the Phe at position 48, strongly contribute to a narrower and more hydrophobic site in AKR1B15, which would be a basic structural feature that accounts for the functional uniqueness of this enzyme within the AKR1B subfamily.

A more compact substrate-binding site may facilitate the activity of AKR1B15 towards both aliphatic ketones and 17-ketosteroids, two very poor substrate types for AKR1B10 but excellent for AKR1B15 [26, 27]. Regarding inhibitors, a previous study showed that JF0064, a compound more hydrophobic and smaller than other inhibitors, fits well in AKR1B15 [27]. In contrast, other inhibitors, such as sorbinil, do not inhibit AKR1B15 because of steric hindrance with Phe48 and Phe301, and Phe304 may prevent tolrestat from binding [27]. The behavior of the AKR1B10 mutants carrying the AKR1B15-specific Phe residues nicely mimics the effect of inhibitors on AKR1B15. Another property, also unique for AKR1B15, is its low solubility in bacterial expression systems. Thus, in the expression and purification of recombinant AKR1B15 using different *E. coli* strains and procedures, the protein appeared mostly in the insoluble fraction of cell lysates. With the co-expression of three chaperone systems the amount of soluble AKR1B15 increased significantly, although most of the protein was still associated with the insoluble fraction [27]. In contrast, both mutants could be purified as soluble proteins, similarly to wild-type AKR1B10. The exchanged residues *per se*, therefore, do not seem to be relevant for the low solubility of AKR1B15.

The present results and novel reports from other groups add further information on the possible physiological function of AKR1B10 and AKR1B15 as retinaldehyde reductases. The existence of a

variety of enzymes that can reduce retinaldehyde is intriguing. At least five enzymes of the short-chain dehydrogenase/reductase (SDR) superfamily are involved in this function [43,44], in addition to the two AKRs studied here, along with some members of the AKR1C subfamily [45]. It has been hypothesized that DHRS3, linked to RDH10, would be the SDR retinaldehyde reductase responsible for the control of the right amount of retinoic acid in the cell [46]. Other reductases may have a more general function in the maintenance of retinoid homeostasis [44]. It is well accepted that important sources of retinol are the carotenoids from the diet [47]. These are centrally cleaved by β-carotene 15,15'-oxygenase (BCO1) to produce two molecules of retinaldehyde, that would be reduced to retinol for storage as retinyl esters. BCO1 is found in the intestine but also in liver and several peripheral tissues where it can act on the significant fraction of carotenoids (and other plant pigments) which can be absorbed uncleaved from the intestine into the blood circulation [48]. An alternative (eccentrical) carotenoid cleavage is catalyzed by β-carotene 9,10-oxygenase (BCO2), and probably by non-enzymatic mechanisms, yielding a variety of apocarotenals and apocarotenones [48]. Several of these compounds and their metabolites exhibit biological activity. We have recently demonstrated that several apocarotenals are oxidized by retinaldehyde dehydrogenases of the ALDH superfamily to their acid forms [49]. It is very plausible that the reduction of the apocarotenals and apocarotenones takes place also *in vivo*, and retinaldehyde reductases would be suitable enzymes for this function. These enzymes exhibit diverse localizations, microsomal (most of the retinoid-associated SDRs), cytosolic (AKR1B10 and AKR1C3), and mitochondrial (RDH13 and AKR1B15), which is compatible with the different localization of the carotenoid metabolism by BCO1 (cytosolic) and BCO2 (mitochondrial).

Moreover, we have demonstrated that AKR1B15 is a very efficient 17-ketosteroid reductase, even more active than AKR1C3 [50,51]. Thus, besides a likely role in retinoid metabolism, AKR1B15 may be also involved in the metabolism of steroid hormones *in vivo*, and its presence in reproductive organs (placenta, ovary, prostate, testis) [26] supports this assumption. Hence, some of the AKR1B15 properties are reminiscent of those of AKR1C3, such as their common tissue localization and specificity for 9-*cis*-retinaldehyde and 17-ketosteroids. The ability of AKR1B15 to convert steroids and its

mitochondrial localization could link the enzyme to hormonal regulation of mitochondrial functions. In this regard, the association of a single-point mutation in AKR1B15 with a severe infantile phenotype with impaired mitochondrial function [28] supports an important role of AKR1B15 in mitochondria, either via steroid activation or via other mechanisms.

In contrast to AKR1B15, the structurally very close AKR1B10 enzyme exhibited only residual activity with C_{18} and C_{19} steroids and, surprisingly, showed higher activity for 17-hydroxysteroid oxidation than 17-ketosteroid reduction. However, the very poor performance with C_{18} and C_{19} steroids makes a role of AKR1B10 in this metabolic pathway under normal physiological conditions very unlikely. In the past, it had been reported that AKR1B10 could not oxidize 17β-hydroxysteroids, while it could oxidize 20α-hydroxysteroids, but with very low activity, and it could be inhibited by estrogenic and androgenic steroids (including estrone, 17β-estradiol, Δ4-androstenedione and testosterone) [7]. The discrepancies between these observations and our results might be explainable by the fact that we specifically analyzed the conversion of steroids using a very sensitive HPLC-based method. With respect to the preferred oxidative activity of AKR1B10 with aromatic compounds, it was previously shown that AKR1B10 oxidizes the *trans*-dihydrodiols of polycyclic aromatic hydrocarbons to their reactive *o*-quinones, which might be a factor contributing to carcinogenesis when AKR1B10 is upregulated [52].

Overall, the members of the AKR and SDR superfamilies are known for their broad and overlapping substrate spectrum, in particular, they share their specificity for retinoids and steroids. Thus, AKR1B10 and AKR1B15 (present work) plus members of the AKR1C subfamily [45,51], as well as several SDRs, i.e., 17β-HSD1 [53] and DHRS7 [54] show activity with both retinoids and steroids. This provides ample opportunity for the participation of these enzymes in hormonal regulation at the pre-receptor level and crosstalk between different signaling pathways.

In conclusion, we have demonstrated that a few amino acid residues, including several Phe that are unique for AKR1B15 and line the substrate-binding site, strongly participate in the distinct substrate

specificity and inhibitor selectivity of AKR1B15, very different from those of AKR1B10, a structurally closely related enzyme. AKR1B15, the most recently described human AKR, exhibits a robust reductase activity towards retinaldehydes and 17-ketosteroids, and thus a role in the metabolism of these and related compounds is proposed.

Conflict of interest

The authors declare that there are no conflicts of interest.

Acknowledgements

This work was funded by the Spanish Ministerio de Economía y Competitividad (BFU2011-24176 and BIO2016-78057). We thank Marion Schieweg for her excellent technical assistance and Raquel Pequerul for her help in editing the manuscript.

Bibliography

[1] O.A. Barski, S.M. Tipparaju, A. Bhatnagar, The aldo-keto reductase superfamily and its role in drug metabolism and detoxification., Drug Metab. Rev. 40 (2008) 553–624.

[2] Y. Jin, T.M. Penning, Aldo-keto reductases and bioactivation/detoxication., Annu. Rev. Pharmacol. Toxicol. 47 (2007) 263–292.

[3] G. Sanli, J.I. Dudley, M. Blaber, Structural biology of the aldo-keto reductase family of enzymes, Cell Biochem. Biophys. 38 (2003) 79–101.

[4] S. Endo, T. Matsunaga, A. Ikari, O. El-Kabbani, A. Hara, Y. Kitade, Identification of a determinant for strict NADP(H)-specificity and high sensitivity to mixed-type steroid inhibitor of rabbit aldo–keto reductase 1C33 by site-directed mutagenesis, Arch. Biochem. Biophys. 569 (2015) 19–25.

[5] B. Crosas, E. Cederlund, D. Torres, H. Jörnvall, J. Farrés, X. Parés, A vertebrate aldo-keto reductase active with retinoids and ethanol., J. Biol. Chem. 276 (2001) 19132–19140.

[6] D. Cao, S.T. Fan, S.S.M. Chung, Identification and Characterization of a Novel Human Aldose Reductase-like Gene., J. Biol. Chem. 273 (1998) 11429–11435.

[7] S. Endo, T. Matsunaga, H. Mamiya, C. Ohta, M. Soda, Y. Kitade, et al., Kinetic studies of AKR1B10, human aldose reductase-like protein: endogenous substrates and inhibition by steroids., Arch. Biochem. Biophys. 487 (2009) 1–9.

[8] H.-J.M. Martin, U. Breyer-Pfaff, V. Wsol, S. Venz, S. Block, E. Maser, Purification and characterization of AKR1B10 from human liver: role in carbonyl reduction of xenobiotics, Drug Metab. Dispos. 34 (2009) 464–470.

[9] Y. Shen, L. Zhong, S. Johnson, D. Cao, Human aldo-keto reductases 1B1 and 1B10: a

comparative study on their enzyme activity toward electrophilic carbonyl compounds., Chem. Biol. Interact. 191 (2011) 192–198.

[10] B. Crosas, D.J. Hyndman, O. Gallego, S. Martras, X. Parés, T.G. Flynn, et al., Human aldose reductase and human small intestine aldose reductase are efficient retinal reductases: consequences for retinoid metabolism., Biochem. J. 373 (2003) 1973–1979.

[11] O. Gallego, F.X. Ruiz, A. Ardèvol, M. Domínguez, R. Alvarez, A.R. de Lera, et al., Structural basis for the high all-trans-retinaldehyde reductase activity of the tumor marker AKR1B10., Proc. Natl. Acad. Sci. U. S. A. 104 (2007) 20764–20769.

[12] E. Zeindl-Eberhart, S. Haraida, S. Liebmann, P.R. Jungblut, S. Lamer, D. Mayer, et al., Detection and Identification of Tumor-Associated Protein Variants in Human Hepatocellular Carcinomas, Hepatology. 39 (2004) 540–549.

[13] H. Tsuzura, T. Genda, S. Sato, A. Murata, Y. Kanemitsu, Y. Narita, et al., Expression of Aldo-Keto Reductase Family 1 Member B10 in the Early Stages of Human Hepatocarcinogenesis, Int. J. Mol. Sci. 15 (2014) 6556–6558.

[14] S. Fukumoto, N. Yamauchi, H. Moriguchi, Y. Hippo, A. Watanabe, J. Shibahara, et al., Overexpression of the Aldo-Keto Reductase Family Protein AKR1B10 Is Highly Correlated with Smokers' Non–Small Cell Lung Carcinomas, Clin. Cancer Res. 11 (2005) 1776–1785.

[15] M.-W. Kang, E.-S. Lee, S.Y. Yoon, J. Jo, J. Lee, H.K. Kim, et al., AKR1B10 is Associated with Smoking and Smoking-Related Non-Small-Cell Lung Cancer, J. Int. Med. Res. 39 (2011) 78–85.

[16] S. Heringlake, M. Hofdmann, A. Fiebeler, M.P. Manns, W. Schmiegel, A. Tannapfel, Identification and expression analysis of the aldo–keto reductase 1B10 gene in primary malignant liver tumours, J. Hepatol. 52 (2010) 220–227.

[17] Y.T. Chung, K.A. Matkowskyj, H. Li, H. Bai, W. Zhang, M.-S. Tsao, et al., Overexpression and oncogenic function of aldo-keto reductase family 1B10 (AKR1B10) in pancreatic carcinoma, Mod. Pathol. 25 (2012) 758–766.

[18] J. Ma, D.-X. Luo, C. Huang, Y. Shen, Y. Bu, S. Markwell, et al., AKR1B10 overexpression in breast cancer: association with tumor size, lymph node metastasis and patient survival and its potential as a novel serum marker., Int. J. Cancer. 131 (2012) 862–871.

[19] C. Huang, S. Verhulst, Y. Shen, Y. Bu, Y. Cao, Y. He, et al., AKR1B10 promotes breast cancer metastasis through integrin α5/δ-catenin mediated FAK/Src/Rac1 signaling pathway, Oncotarget. 7 (2016) 43779–43791.

[20] C. Huang, Z. Cao, J. Ma, Y. Shen, Y. Bu, R. Khoshaba, et al., AKR1B10 activates diacylglycerol (DAG) second messenger in breast cancer cells, Mol. Carcinog. 57 (2018) 1300–1310.

[21] J. Breton, M.C. Gage, A.W. Hay, J.N. Keen, C.P. Wild, C. Donnellan, et al., Proteomic screening of a cell line model of esophageal carcinogenesis identifies cathepsin D and aldo-keto reductase 1C2 and 1B10 dysregulation in Barrett's esophagus and esophageal adenocarcinoma, J. Proteome Res. 7 (2008) 1953–1962.

[22] H. Yoshitake E, M. Takahashi, H. Ishikawa, M. Nojima, H. Iwanari, A. Watanabe, et al., Aldo-keto reductase family 1, member B10 in uterine carcinomas: a potential risk factor of recurrence after surgical therapy in cervical cancer, Int. J. Gynecol. Cancer. 17 (2007) 1300–1306.

[23] Y.-C. He, Y. Shen, Y. Cao, F.-Q. Tang, D.-F. Tian, C.-F. Huang, et al., Overexpression of AKR1B10 in nasopharyngeal carcinoma as a potential biomarker, Cancer Biomarkers. 16 (2016) 127–135.

[24] N. Jumper, T. Hodgkinson, G. Arscott, Y. Har-Shai, R. Paus, A. Bayat, The Aldo-Keto

Reductase AKR1B10 Is Up-Regulated in Keloid Epidermis, Implicating Retinoic Acid Pathway Dysregulation in the Pathogenesis of Keloid Disease, J. Invest. Dermatol. 136 (2016) 1500–1512.

[25] J.K. Salabei, X.-P. Li, J.M. Petrash, A. Bhatnagar, O.A. Barski, Functional expression of novel human and murine AKR1B genes., Chem. Biol. Interact. 191 (2011) 177–184.

[26] S. Weber, J.K. Salabei, G. Möller, E. Kremmer, A. Bhatnagar, J. Adamski, et al., Aldo-Keto Reductase 1B15 (AKR1B15): a Mitochondrial Human Aldo-Keto Reductase with Activity towards Steroids and 3-Keto-acyl-CoA Conjugates, J. Biol. Chem. 290 (2015) 6531–6545.

[27] J. Giménez-Dejoz, M.H. Kolář, F.X. Ruiz, I. Crespo, A. Cousido-Siah, A. Podjarny, et al., Substrate Specificity, Inhibitor Selectivity and Structure-Function Relationships of Aldo-Keto Reductase 1B15: A Novel Human Retinaldehyde Reductase, PLoS One. 10 (2015) e0134506.

[28] S.E. Calvo, A.G. Compton, S.G. Hershman, S.C. Lim, D.S. Lieber, E.J. Tucker, et al., Molecular diagnosis of infantile mitochondrial disease with targeted next-generation sequencing., Sci. Transl. Med. 4 (2012) 118ra10.

[29] J. Reumers, P. De Rijk, H. Zhao, A. Liekens, D. Smeets, J. Cleary, et al., Optimized filtering reduces the error rate in detecting genomic variants by short-read sequencing., Nat. Biotechnol. 30 (2012) 61–68.

[30] X. Robert, P. Gouet, Deciphering key features in protein structures with the new ENDscript server, Nucleic Acids Res. 42 (2014) 320–324.

[31] M. Biasini, S. Bienert, A. Waterhouse, K. Arnold, G. Studer, T. Schmidt, et al., SWISS-MODEL: Modelling protein tertiary and quaternary structure using evolutionary information, Nucleic Acids Res. 42 (2014) 1–7.

[32] J.D. Durrant, C.A.F. de Oliveira, J.A. McCammon, POVME: an algorithm for measuring binding-pocket volumes., J. Mol. Graph. Model. 29 (2011) 773–776.

[33] O. Gallego, O. V Belyaeva, S. Porté, F.X. Ruiz, A. V Stetsenko, E. V Shabrova, et al., Comparative functional analysis of human medium-chain dehydrogenases, short-chain dehydrogenases/reductases and aldo-keto reductases with retinoids., Biochem. J. 399 (2006) 101–109.

[34] V. Kuksa, Y. Imanishi, M. Batten, K. Palczewski, A.R. Moise, Retinoid cycle in the vertebrate retina: experimental approaches and mechanisms of isomerization., Vision Res. 43 (2003) 2959–2981.

[35] O. V Belyaeva, O. V Korkina, A. V Stetsenko, T. Kim, P.S. Nelson, N.Y. Kedishvili, Biochemical properties of purified human retinol dehydrogenase 12 (RDH12): catalytic efficiency toward retinoids and C9 aldehydes and effects of cellular retinol-binding protein type I (CRBPI) and cellular retinaldehyde-binding protein (CRALBP) on the oxi, Biochemistry. 44 (2005) 7035–7047.

[36] E. Calam, S. Porté, M.R. Fernández, J. Farrés, X. Parés, J.A. Biosca, Biocatalytic production of alpha-hydroxy ketones and vicinal diols by yeast and human aldo-keto reductases., Chem. Biol. Interact. 202 (2013) 195–203.

[37] J. Giménez-Dejoz, S. Weber, O.A. Barski, G. Möller, J. Adamski, X. Parés, et al., Characterization of AKR1B16, a novel mouse aldo-keto reductase, Chem. Biol. Interact. 276 (2017) 182–193.

[38] F.X. Ruiz, Aldo-ceto reductases humanes de les subfamílies AKR1B i AKR1C: activitat amb retinoides i cerca d'inhibidors, Universtitat Autònoma de Barcelona, 2010.

[39] S. Endo, T. Matsunaga, K. Kuwata, H.-T. Zhao, O. El-Kabbani, Y. Kitade, et al., Chromene-3-carboxamide derivatives discovered from virtual screening as potent

inhibitors of the tumour maker, AKR1B10., Bioorg. Med. Chem. 18 (2010) 2485–90.

[40] A. Cousido-Siah, F.X. Ruiz, A. Mitschler, S. Porté, A.R. De Lera, M.J. Martín, et al., Identification of a novel polyfluorinated compound as a lead to inhibit the human enzymes aldose reductase and AKR1B10: Structure determination of both ternary complexes and implications for drug design, Acta Crystallogr. Sect. D Biol. Crystallogr. 70 (2014) 889–903.

[41] M. Takemura, S. Endo, T. Matsunaga, M. Soda, H.-T. Zhao, O. El-Kabbani, et al., Selective inhibition of the tumor marker aldo-keto reductase family member 1B10 by oleanolic acid., J. Nat. Prod. 74 (2011) 1201–6.

[42] A. Cousido-Siah, F.X. Ruiz, I. Crespo, S. Porté, A. Mitschler, X. Parés, et al., Structural analysis of sulindac as an inhibitor of aldose reductase and AKR1B10, Chem. Biol. Interact. 234 (2015) 290–6.

[43] N.Y. Kedishvili, Enzymology of retinoic acid biosynthesis and degradation, J. Lipid Res. 54 (2013) 1744–1760.

[44] O. V. Belyaeva, L. Wu, I. Shmarakov, P.S. Nelson, N.Y. Kedishvili, Retinol dehydrogenase 11 is essential for the maintenance of retinol homeostasis in liver and testis in mice, J. Biol. Chem. 293 (2018) 6996–7007.

[45] F.X. Ruiz, S. Porté, O. Gallego, A. Moro, A. Ardèvol, A. Del Río-Espínola, et al., Retinaldehyde is a substrate for human aldo–keto reductases of the 1C subfamily, Biochem. J. 440 (2011) 335–344.

[46] O. V. Belyaeva, M.K. Adams, L. Wu, N.Y. Kedishvili, The antagonistically bifunctional retinoid oxidoreductase complex is required for maintenance of all-trans-retinoic acid homeostasis, J. Biol. Chem. 292 (2017) 5884–5897.

[47] W.S. Blaner, Y. Li, P.J. Brun, J.. Yuen, S.. Lee, R.D. Clugston, Vitamin A absorption,

storage and mobilization, in: M. Asson-Batres, C. Rochette-Egly (Eds.), Biochem. Retin. Signal. II. Subcell. Biochem., Springer, Dordrecht, 2016: pp. 95–125.

[48] E.H. Harrison, L. Quadro, Apocarotenoids: Emerging Roles in Mammals, Annu. Rev. Nutr. 38 (2018) 153–172.

[49] M. Domínguez, R. Pequerul, R. Alvarez, J. Giménez-Dejoz, E. Birta, S. Porté, et al., Synthesis of apocarotenoids by acyclic cross metathesis and characterization as substrates for human retinaldehyde dehydrogenases, Tetrahedron. 74 (2018) 2567–2574.

[50] T.M. Penning, S. Steckelbroeck, D.R. Bauman, M.W. Miller, Y. Jin, D.M. Peehl, et al., Aldo-keto reductase (AKR) 1C3: Role in prostate disease and the development of specific inhibitors, Mol. Cell. Endocrinol. 248 (2006) 182–191.

[51] T.M. Penning, M.E. Burczynski, J.M. Jez, C.F. Hung, H.K. Lin, H. Ma, et al., Human 3α-hydroxysteroid dehydrogenase isoforms (AKR1C1-AKR1C4) of the aldo-keto reductase superfamily: functional plasticity and tissue distribution reveals roles in the inactivation and formation of male and female sex hormones., Biochem. J. 351 (2000) 67–77.

[52] A.M. Quinn, R.G. Harvey, T.M. Penning, Oxidation of PAH trans-dihydrodiols by human aldo-keto reductase AKR1B10, Chem. Res. Toxicol. 21 (2008) 2207–2215.

[53] F. Haller, E. Moman, R.W. Hartmann, J. Adamski, R. Mindnich, Molecular framework of steroid/retinoid discrimination in 17β-hydroxysteroid dehydrogenase type 1 and photoreceptor-associated retinol dehydrogenase, J. Mol. Biol. 399 (2010) 255–267.

[54] H. Štambergová, L. Zemanová, T. Lundová, B. Malčeková, A. Skarka, M. Šafr, et al., Human DHRS7, promising enzyme in metabolism of steroids and retinoids?, J. Steroid Biochem. Mol. Biol. 155 (2016) 112–119.